P. E. V. de Miranda and R. Pascual†*

Initial Stages of Hydrogen Induced Short Fatigue Crack Propagation

REFERENCE de Miranda, P. E. V. and Pascual, R., **Initial Stages of Hydrogen Induced Short Fatigue Crack Propagation**, *The Behaviour of Short Fatigue Cracks*, EGF Pub. 1 (Edited by K. J. Miller and E. R. de los Rios) 1986, Mechanical Engineering Publications, London, pp. 179–190.

ABSTRACT The initiation of fatigue cracks was studied in an austenitic stainless steel type AISI 304L which was cathodically hydrogenated, outgassed, and then tested. Tests were conducted with R ratio equal to -1 at 30 Hz and stopped at different periods of the fatigue life to permit a survey of the gauge surface of the samples with a scanning electron microscope.

Contrary to the non-hydrogenated fatigued material, slip marks were not evident on the surface of the hydrogenated and outgassed samples. From the beginning of the fatigue life the gauge surface exhibited a 'peeling off' of very thin layers in several regions which was always associated with pre-existing hydrogen-induced cracks.

However, the main fatigue crack was found to initiate sub-superficially probably in the region close to the interface between the hydrogen hardened outermost layer and the inside ductile material. Since the hydrogen-induced surface cracks do not grow themselves, they are not likely to be used as a tool to model the fatigue behaviour of short cracks in austenitic stainless steels.

Introduction

The introduction of hydrogen into the structure of austenitic steels may harm their mechanical properties if they are not outgassed at a high enough temperature, or if mechanical work is applied while hydrogen is still in the material. There is a broad variety of situations in which austenitic stainless steels are used in hydrogen rich environments, especially in the chemical and nuclear industries. These steels are particularly affected by the presence of hydrogen if outgassing takes place at around room temperature (**1**). The low diffusion coefficient of hydrogen in austenite (as compared to the mobility it has in ferrite) leads to an accumulation of a high content of hydrogen in a very superficial layer of the material. As a result, high localized levels of strain are developed (as was shown by the use of X-ray techniques (**1**)–(**6**)) and the following surface effects might be observed, depending on the chemical composition of the steel and the consequent level of austenite instability: (i) during hydrogenation austenite may destabilize and transform partially into an h.c.p. ε martensitic phase; (ii) upon outgassing another martensitic transformation may take place (giving rise to an α' phase) as well as the appearance of very small superficial cracks. Both nucleate and grow with time after hydrogenation, i.e., with ageing time, and, in fact, the b.c.c. α' martensitic phase will occur

* COPPE-EE-Universidade Federal do Rio de Janerio, C.P. 68505 – CEP 21945 Rio de Janeiro, RJ – Brazil.

† Instituto Militar de Engenharia – Praça Gal. Tibúrcio, 80, CEP: 22290 Rio de Janeiro, RJ – Brazil.

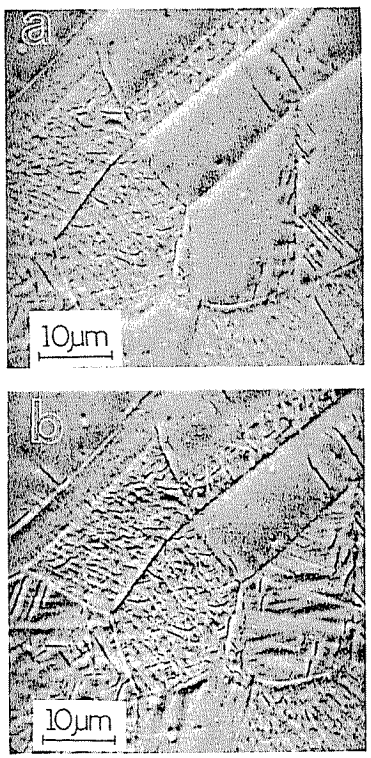

Fig 1 Delayed features associated with the room temperature outgassing of a hydrogenated austenitic stainless steel. Bulged grains, such as in (a), and the delayed appearance of cracks and a martensitic phase, as in (b). Micrographs were made (a) 30 minutes, and (b) 20 hours after hydrogenation. Unetched (7)

preferentially close to the delayed cracks due to the high concentration of deformation at these regions (7). Figure 1 shows an example of the delayed appearance of cracks and phase transformation for an AISI type 304L stainless steel degassed at room temperature. The same area was photographed 30 minutes (Fig. 1(a)) and 20 hours (Fig. 1(b)) after hydrogenation. The kinetics of phase and crack appearance varies from grain to grain. It is also interesting to take into account the fact that the hydrogenated samples show an increase in surface hardening (**8**).

The effect of hydrogen contained in the material and that of the surface effects induced by hydrogen in austenite have been studied in uniaxial tension (**9**)–(**13**). It was found that hydrogen may indeed cause a severe decrease in the ductility of austenite, but the effect is more pronounced in very thin samples due to the very low diffusion coefficient of hydrogen in austenite. That is, the mechanical properties in tension depend on the geometry of the hydrogenated sample, since higher values of surface to volume ratio increases the susceptibility to hydrogen embrittlement (**12**)(**14**). Tensile testing of outgassed samples, which contain surface cracks and martensitic phases, showed that the material recovers most of its ductility (**12**)(**15**). This indicated both the presence of hydrogen in the structure to cause the embrittlement of the austenite, and that the hydrogen-induced surface effects in this material are of secondary importance when considering the mechanical properties in uniaxial tension. However, the question of how these hydrogen induced surface effects (specially the delayed cracks) would influence the fatigue properties of austenitic steels, which are influenced by surface conditions, should be addressed.

Table 1 Number of cracks (N) per square millimetre as a function of the current density (J) used for a two-hour cathodic hydrogenation of 304 stainless steel at room temperature (14)

J (Amps/m^2)	50	250	500	1000	2000	4000	10 000
N (mm$^{-2} \times 10^{-3}$)	85.2	138.9	177.8	216.7	259.3	307.4	305.6

The first step towards answering this question involved the morphological and quantitative characterization of these surface cracks (**2**)(**6**)(**7**)(**14**)(**16**)–(**19**), which showed that the cracks are very small (having average length smaller than one grain diameter) and very shallow due to the small depth of penetration of hydrogen into the austenite. They appear in a crystallographic fashion, with different orientations in different grains, and are numerous, as is exemplified by the results shown in Table 1. As a summary of the results obtained to date, it is widely accepted that: (a) the depth of the hydrogen-induced cracks in austenitic stainless steel and of the hardened layer, measured by metallographic sectioning, was found to be of the order of 6 to 15 μm (**14**)(**17**), 20 μm (**5**) or even 50 μm (**2**) depending on the current density, time, and temperature of charging, as well as on the alloy's chemical composition and microstructure; (b) a compressive stress state was found to occur on the surface of the sample during charging, which, coupled with tensile stress during outgassing, lead to phase transformations, plastic deformation, and cracking (**4**)–(**7**)(**16**); (c) the number of cracks differs widely from grain to grain (**2**)(**5**)(**6**)–(**8**)(**16**), but may reach average densities of thousands of cracks per square millimetre (Table 1 and references (**14**) and (**18**)).

The second step was to conduct fatigue tests of hydrogen charged and outgassed samples. These showed (**8**) that the fatigue life of type AISI 304 stainless steel was reduced about 40 per cent by a hydrogenation–outgassing cycle, due to the introducton of surface cracks. The effect was more significant for high cycle fatigue conditions. It was also observed that the fatigue fracture surface presented steps, whereas the non-hydrogenated specimens had a fairly flat overall fracture surface. This was rationalized as a function of the simultaneous growth of different hydrogen-induced surface cracks during fatiguing. It was then realized that these facts would be better understood by studying the initiation phenomenon of the fatigue cracks on the hydrogenated and outgassed samples. This is one of the objectives of the present paper. Another objective

is to analyse the possibility of using hydrogen-induced surface cracks, which can be introduced in a controlled way, to model the fatigue behaviour of short cracks in an austenitic stainless steel.

Experimental procedures

A hot rolled sheet of an AISI type 304L stainless steel with a thickness of about 4.0 mm was used in this work, having the following chemical composition (wt%): C 0.024, Cr 18.25, Ni 9.50, Mn 1.37, Si 0.51, P 0.037, S 0.006, Mo 0.060, N 0.0379, Fe balance. Flat hour-glass type fatigue specimens with a 20 mm minimum gauge width and a 7 mm gauge radius of curvature were machined parallel to the rolling direction and then heat treated for 30 minutes at 1100°C and quenched in water. This yielded a mean grain size of 74.4 μm (Fig. 2(a)) and a hardness of 148 Vickers. All microhardness measurements were taken with a load of 50 g. The static mechanical properties of this material were: yield stress: 208.90 MPa, tensile strength: 678.80 MPa, elongation: 79.8 per cent.

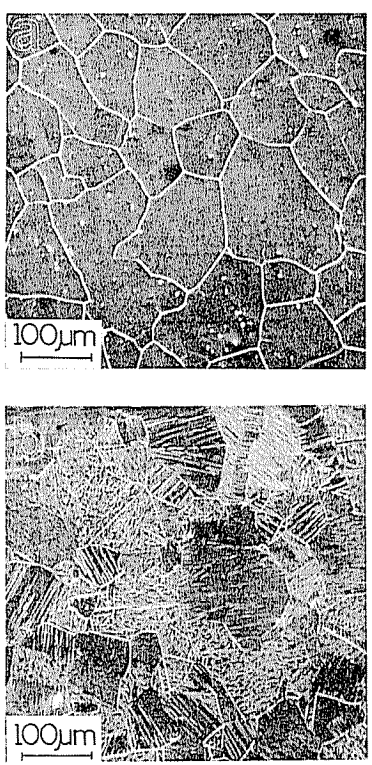

Fig 2 Initial microstructure of the material. (a) Non-hydrogenated. Electrolytically etched with 50 per cent H_2O + 50 per cent HNO_3, J = 4402 amps/m^2, t = 90 s at room temperature (b) Hydrogenated and outgassed. Unetched

Hydrogenation was performed cathodically at room temperature, using an electrolyte of H_2SO_4 1 N containing 100 mg/l of As_2O_3, for 4 hours and with a current density of 1000 A/m^2. After hydrogenation the samples were aged at room temperature and atmospheric pressure for one week before testing, which gave rise to surface cracks and to martensitic phases (Fig. 2(b)) as most of the hydrogen introduced by the electrolitic charging was outgassed. The hardness of the hydrogenated and outgassed sample was 192 Vickers.

Fatigue tests were conducted at room temperature, in a servo-hydraulic machine in tension–compression, at a frequency of 30 Hz and R ratio of -1.

The initiation and growth of fatigue cracks was studied in constant stress range tests, which were interrupted at several points during the fatigue life in order to survey the lateral surfaces of the gauge section with a scanning electron microscope.

Results

All the results selected to describe the fatigue behaviour in this paper

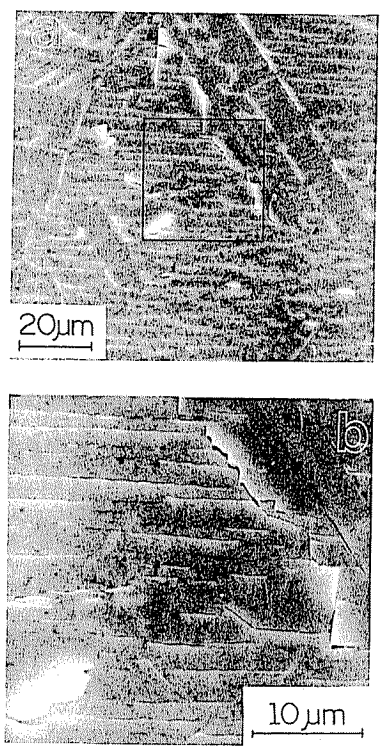

Fig 3 Detail of the gauge surface of a hydrogenated–outgassed sample fatigued to 15 per cent of its fatigue life. (b) shows an enlargement of the area indicated in (a). Unetched

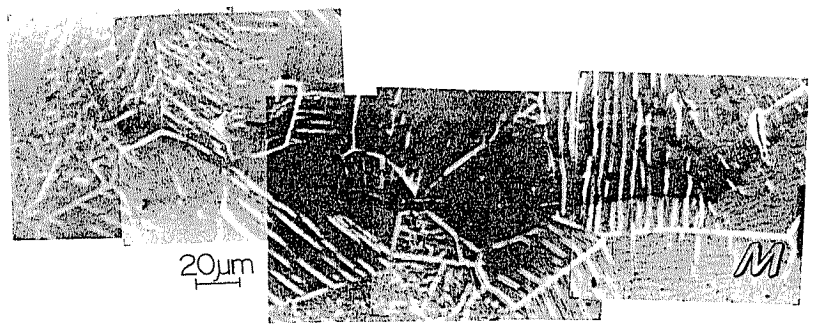

Fig 4 Early indication of the fatigue sub-surface crack appearing on the surface of the hydrogenated and outgassed sample at 49 per cent of its fatigue life. Unetched

correspond to a constant maximum stress of 195 MPa. For this condition the fatigue life of the non-hydrogenated specimens was found to be 317 000 cycles, while that of the hydrogenated–outgassed samples was 101 000 cycles, which corresponds to about 32 per cent of the former.

The first effect that could be observed on the surface of the hydrogenated and outgassed fatigued samples was the 'peeling off' of very thin layers in several small regions throughout the gauge section. This is depicted in Fig. 3(a) and (b) and gives the impression of being due to the fracture of very fragile parts of the outermost surface and associated with the pre-existent hydrogen-induced microcracks. These fractured regions appear whiter in the micrographs because they stand up above the plane of the surface. They show up immediately after a few fatigue cycles and remain without much change throughout the fatigue life. Some of these fractured zones, however, eventually fall off the surface. The hydrogen induced microcracks were not observed to grow in length throughout the fatigue life.

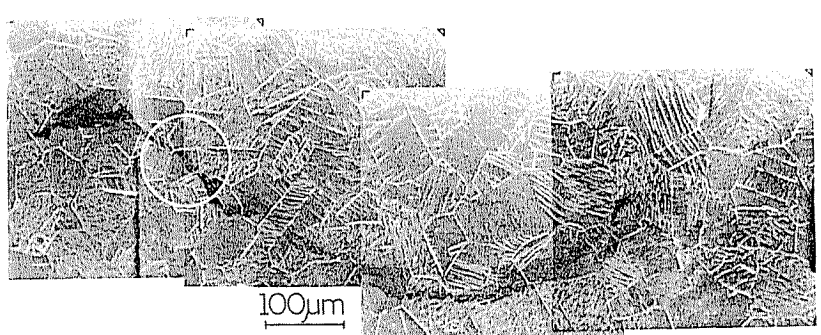

Fig 5 Growth of the feature associated with the sub-surface fatigue crack for the hydrogenated and outgassed specimen at 63 per cent of its fatigue life. The area shown in Fig. 4 is included. Unetched

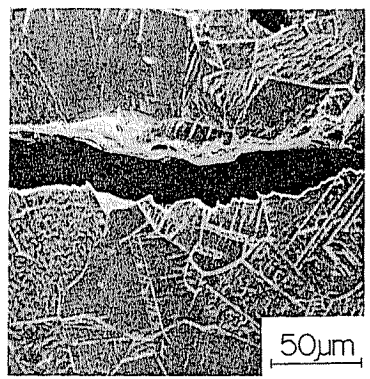

Fig 6 Fatigue crack on the gauge lateral surface at the termination of fatigue life of a hydrogenated and outgassed sample. This micrograph corresponds to the area indicated by the white circle in Fig. 5. Unetched

In all the specimens observed, the main fatigue crack developed in the way represented in Figs 4, 5, and 6, which correspond to the same region of the surface of a particular specimen. Some dark markings, such as the one shown in Fig. 4, were found to appear on the gauge surface of the specimens and grow in length with increasing number of fatigue cycles. One of the marks was always found to be associated with the main fatigue crack responsible for fracture (Fig. 6). In brief, the main crack developed sub-surface and was visible at first as a dark marking on the surface. Only by the end of the fatigue life did the main fatigue crack open to show a crack on the surface. The sub-surface crack depicted in Fig. 4 was photographed after the sample was cycled 49 per cent of its fatigue life. It is interesting to note that it spread transgranularly, crossing without distinction grains with and without hydrogen-induced surface cracks, and did not follow the direction of these cracks, so that it cannot be thought to be formed mainly as a consequence of the in-depth growth of hydrogen-induced cracks. The same sub-surface crack of Fig. 4 has grown much longer after cycling the sample about 63 per cent of the fatigue life as shown in the micrograph of Fig. 5. In both Fig. 4 and Fig. 5 the white markings (white lines) represent the sites where there are intergranular and transgranular hydrogen-induced surface cracks. In a few regions of Fig. 4 (which was taken with greater magnification) the martensitic phase (marked M) can be noted. No relationship between this phase and the sub-surface cracks was found. Finally, Fig. 6 shows the crack at the end of the fatigue life in the same region circled in Fig. 5.

The fracture surface in the region appearing on the upper left side of Fig. 5 is shown in Fig. 7. It is interesting to observe that that hump in the sub-surface crack appearing on the upper left hand side of Fig. 5 (to the left of the white circle) corresponds exactly to the step found on the fracture surface shown in Fig. 7. A detail of the top part of this step, closer to the surface of the sample (on the left hand side of Fig. 7) is presented in Fig. 8. This micrograph shows

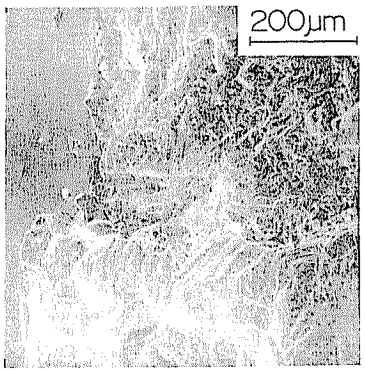

Fig 7 Detail of a step on the fracture surface of a fatigued hydrogenated–outgassed sample. The step corresponds to the hump on the upper left hand side in Fig. 5

the presence of secondary cracks, one of which appears to start from what may be a hydrogen-induced surface crack (marked C in Fig. 8). S.E.M. observations included careful examination of the lateral and of the fracture surfaces of the hydrogenated–outgassed samples. Despite this, no clear indication of initiation sites for the main fatigue crack was found, probably due to the fact that the fracture surfaces are very irregular.

It was not an objective of this paper to give a detailed analysis of the initiation and propagation features of the fatigue crack in the non-hydrogenated material. However, for the sake of comparison with the hydrogenated–outgassed samples, Fig. 9 shows the features associated with the propagation of a fatigue crack in a non-hydrogenated specimen tested under the same conditions of the former. A great number of slip marks can be observed.

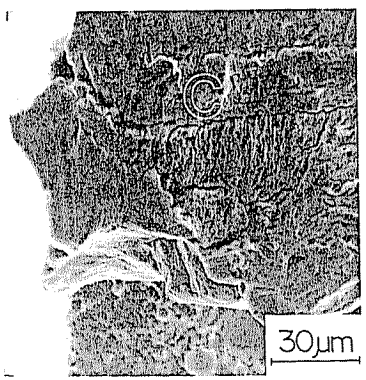

Fig 8 Magnification of a region of Fig. 7 at the top of the step on the fracture morphology, near to the lateral surface of a fatigued hydrogenated–outgassed sample. A fatigue crack is marked at C

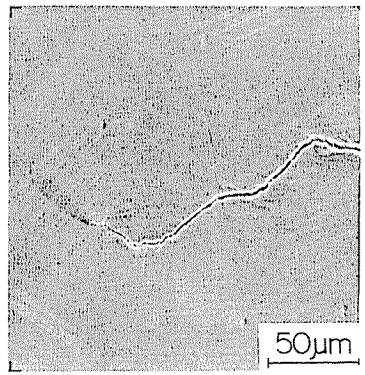

Fig 9 A fatigue crack on the lateral gauge surface of a non-hydrogenated sample. The micrograph shows many slip marks due to accumulated fatigue strain. Unetched

Discussion

The initiation (**20**)–(**22**) and propagation (**23**) of fatigue cracks in austenitic stainless steels and other f.c.c. materials have been studied recently. It was found that deformation markings appear early in the fatigue life, together with a certain level of surface roughness, and are followed by the nucleation of superficial microcracks. These microcracks grow in number and length and coalesce to form the main fatigue crack. The same behaviour is shown in Fig. 9, relative to fatigued, non-hydrogenated samples.

The fatigue behaviour of the hydrogenated and outgassed specimens was found to be quite different. To begin with, for the conditions used in the present work, no slip markings were evident on the surface, even at fracture, so that there is no evidence of plastic deformation on the surface layer. Also, no nucleation of fatigue microcracks on the surface and/or growth of the pre-existing hydrogen-induced cracks was observed throughout the fatigue life.

Surprisingly, the fatigue cracks were found to initiate sub-surface and not as a result of the growth and coalescence of the pre-existing hydrogen-induced cracks, as was expected. Several factors may influence the initiation of the fatigue cracks, such as the existence of a hardened surface layer, the presence of hydrogen-induced surface cracks, and martensitic phases, as well as the role played by the 'peeled off' areas. The hydrogen-induced hardened surface layer may have an irregular depth due to the fact that the penetration of hydrogen into the material varies greatly according to the local microstructure. The mean depth can be estimated for the present hydrogenation condition as follows. The diffusion coefficient (D) of hydrogen in austenite at 296K can be taken to have the value of 1.38×10^{-16} m^2/s (**24**). The solution of Fick's law for the diffusion in a semi-infinite solid is

$$\frac{C}{C_o} = 1 - \text{erf}\left\{\frac{x}{2\sqrt{(Dt)}}\right\} \quad (1)$$

where C_o is the concentration of hydrogen in the surface, C is the concentration at a depth x, and t is the time of hydrogenation (equal to 14 400 s for the present case). Assuming that the hydrogen-affected region of the material extends to a depth in which the hydrogen concentration is 0.1 per cent of that found in the surface (i.e., $C/C_o = 0.001$), and applying the present conditions in Equation (1), one obtains an average depth of the order of 6 μm which is of the same order of magnitude of the experimental determinations **(2)(5)(14)(17)** mentioned before. This reiterates the opinion that the effects induced by hydrogen are indeed concentrated in a very thin hardened surface layer. The hydrogenated–outgassed specimens behave, then, as a 'composite material', having a hard and thin surface layer, which contains microcracks, surrounding a ductile core. This layer cannot accommodate, plastically, the strains imposed during the fatigue test and the layer fractures locally along the pre-existing hydrogen-induced cracks. However, this effect is not found to be associated with the initiation or growth of the main fatigue crack. This 'peeling off' effect produced a reduction in the effective cross-section of the sample, but this is too small to explain the observed reduction of the fatigue life. This situation is similar to what is observed in a shot-peened material, but with the difference that in the latter the presence of a hardened surface layer usually improves the fatigue life. In both cases the fatigue crack initiates sub-surface. The hydrogen-induced hardened layer differs from the shot-peened one in at least two aspects. One is the presence of delayed surface cracks and the other is the probable irregularity of the depth profile of this layer, due to microstructural inhomogeneities.

Differences in the microstructure of the steel (such as grain and twin boundaries, second phase particles, slip bands, and localized constitutional segregation) makes hydrogen penetration heterogeneous and gives rise, upon outgassing, to a hardened surface layer with an irregular depth profile, as mentioned earlier. This, in turn, could facilitate the nucleation of fatigue sub-surface cracks in several sites close to the interface between the hardened layer and the ductile material inside. For that reason the initiation of the fatigue cracks would be faster in hydrogenated–outgassed samples than in the non-hydrogenated ones. This may have led to the observed decrease in the fatigue life.

On the other hand, even if the pre-existing hydrogen cracks are found not to grow during the fatigue life, they could eventually be responsible for the nucleation of secondary fatigue cracks, which may, in turn, grow and coalesce to form the main crack. In effect, the crack marked C in Fig. 8 seems to have been initiated in a hydrogen-induced surface crack. This effect may also explain the observed reduction in fatigue life. Despite the fact that the initiation sites for the main fatigue crack were not clearly defined, two possibilities are raised

to account for this initiation: (1) the irregular depth profile of the hardened layer, and (2) the stress concentration at the tip of the hydrogen-induced surface cracks. Eventually, they may contribute separately or simultaneously to the decrease in the fatigue life. The existence of multiple secondary fatigue cracks alters the path of the main fatigue crack, which may become wavy, as the one shown in Figs 4 and 5. That is probably why there are features such as the hump on the left hand side of Fig. 5, which gives rise to the steps on the fracture morphology. Finally, due to the complexity of the initiation features in this material, it would not be appropriate to use hydrogen-induced surface cracks as a tool to model the fatigue behaviour of short cracks in austenitic stainless steels.

Conclusions

(1) The short fatigue cracks in the hydrogenated–outgassed material were found to initiate sub-surface.
(2) The fact that the hydrogen-induced surface cracks do not grow themselves eliminates the possibility of using them to model the fatigue behaviour of short cracks in austenitic stainless steels.

Acknowledgements

The authors acknowledge the financial support, which made this research possible, through FINEP, CNPq (Grant No. 402289/84-MM) and Ministério do Exército. Thanks are also expressed to Oswaldo Pires Filho for technical support.

References

(1) NARITA, N., ALTSTETTER, C. J., and BIRNBAUM, H. K. (1982) Hydrogen-related phase transformations in austenitic stainless steels, *Metal. Trans*, **13A**, 1355–1365.
(2) HOLZWORTH, M. L. and LOUTHAN Jr., M. R. (1968) Hydrogen-induced phase transformations in type 304-L stainless steels, *Corrosion–Nace*, **24**, 110–124.
(3) MATHIAS, H., KATZ, Y., and NADIV, S. (1978) Hydrogenation effects in austenitic steels with different stability characteristics, *Metal Sci.*, **00**, 129–137.
(4) TOUGE, M., MIKI, T., and IKEYA, M. (1983) Effects of X-ray irradiation on hydrogen-induced phase transformations in stainless steel, *Met. Trans*, **14A**, 151–152.
(5) BRICOUT, J. P. (1984) *Contribution a l'etude de la fragilisation par l'hidrogene des aciers inoxydables austenitiques instables*, Ph.D thesis, Université de Valenciennes et du Hainaut Cambresis, France.
(6) MIRANDA, P. E. V., SAAVEDRA, A., and PASCUAL, R. (1986) Metallographic characterization of hydrogen-induced surface phenomena in an austenitic stainless steel, *Microstructural science*, **13** (Edited by Shiels, S. A., Bagnall, C., Witkowski, R. E., and Vander Voort, G. F.), (IMS, ASM), pp. 349–359.
(7) DE MIRANDA, P. E. V. (1984) Fenomenologia da fratura retardada e das transformações de fases na austenita hidrogenada, *Proceedings of the VI CBECIMAT*, Rio de Janeiro, pp. 62–67.
(8) PIERANTONI, P. S., MIRANDA, P. E. V., and PASCUAL, R. (1985) Effect of surface cracks induced by hydrogen on the fatigue properties of AISI 304 stainless steel, *Proceedings of the 7th ICSMA*, Montreal, pp. 1213–1218.

(9) HÄNNINEN, H. E. and HAKKARAINEN, T. J. (1980) Influence of metallurgical factors on hydrogen-induced brittle fracture in austenitic stainless steels, *Advances in fracture research* (Edited by Francois, D. *et al.*), (Pergamon Press, Oxford), pp. 1881–1888.
(10) HABASHI, M. and GALLAND, J. (1982) Considérations sur la fragilisation par l'hydrogène des aciers inoxidables austénitiques, *Mem. Etudes Sci. Rev. Met.*, pp. 311–323.
(11) ROSENTHAL, Y., MARK-MARKOWITCH, M., STERN, A., and ELIEZER, D. (1984) Tensile flow and fracture behaviour of austenitic stainless steels after thermal aging in a hydrogen atmosphere, *Mat. Sci. Engng*, **67**, 91–107.
(12) LELÉ, M. V. and DE MIRANDA, P. E. V. (1984) Fragilização e Encruamento do Aço Inoxidável AISI 304 Hidrogenado, *Metalurgia ABM*, **40**, 673–678.
(13) HUWART, P., HABASHI, M., FIDELLE, J. P., GARNIER, P., and GALLAND, J. (1985) Proprietés mechaniques d'aciers inoxydables austenitiques stable (ZXNCTD 26-15) et instable (Z 2 CN 18-10). Role des traitements thermiques et de l'hydrogene cathodique, *Proceedings of the 7th ICSMA*, Montreal, pp. 1099–1104.
(14) SILVA, T. C. V., PASCUAL, R., and DE MIRANDA, P. E. V. (1984) Hydrogen induced surface effects on the mechanical properties of type 304 stainless steel, *Fracture prevention in energy and transport systems* (Edited by Le May, I., and Monteiro, S. N.), (EMAS), pp. 511–520.
(15) WHITEMAN, M. B. and TROIANO, A. R. (1965) Hydrogen embrittlement of austenitic stainless steel, *Corrosion*, **21**, 53–56.
(16) WASIELEWSKI, R. C. and LOUTHAN Jr, M. R. (July 1983) Hydrogen embrittlement of type 316 stainless steel, *Proceedings of the 16th Annual IMS Meeting*, Calgary, Canada.
(17) EVANGELISTA, G. E. and DE MIRANDA, P. E. V. (1984) Efeitos superficiais provocados pelo hidrogênio no aço AISI 304, *Metalurgia ABM*, **40**, 501–506.
(18) SILVA, T. C. V. and DE MIRANDA, P. E. V. (1985) Caracterização das microtrincas induzidas pelo hidrogênio no aço inoxidável austenítico, *Proceedings of the 40th Annual ABM Meeting*, pp. 79–94.
(19) TÄHTINEN, S., KIVILAHTI, J., and HÄNNINEN, H. (1985) Crystallography of hydrogen-induced surface cracking in a spherical austenitic stainless steel crystal, *Scripta Met.*, **19**, 967–972.
(20) CHANG, N. S. and HAWORTH, W. L. (1985) Fatigue crack initiation and early growth in an austenitic stainless steel, *Proceedings of the 7th ICSMA*, Montreal, pp. 1225–1230.
(21) SIGLER, D., MONTPETIT, M. C., and HAWORTH, W. L. (1983) Metallography of fatigue crack initiation in an overaged high-strength aluminium alloy. *Met. Trans*, **14A**, 931–938.
(22) BASINSKI, Z. S. and BASINSKI, S. J. (1985) Low amplitude fatigue of copper single crystals-II. Surface observations, *Acta Met.*, **33**, 1307–1317.
(23) SCHUSTER, G. and ALTSTETTER, C. (1983) Fatigue of stainless steel in hydrogen, *Met. Trans*, **14A**, 2085–2090.
(24) LOUTHAN, M. R. and DERRICK, R. G. (1975) Hydrogen transport in austenitic stainless steel, *Corrosion Sci.*, **15**, 565–577.